Astronomy & Astrophysics manuscript no.
(will be inserted by hand later)

arXiv:astro-ph/0111563v1 29 Nov 2001

Molecular gas at intermediate redshifts

Nissim Kanekar[1⋆], Jayaram N Chengalur[1⋆⋆]

National Centre for Radio Astrophysics, Post Bag 3, Ganeshkhind, Pune 411 007

Received mmddyy/ accepted mmddyy

Abstract. We present Giant Metrewave Radio Telescope (GMRT) observations of OH absorption in B3 1504+377 ($z \sim 0.673$) and PKS 1413+135 ($z \sim 0.247$). OH has now been detected in absorption towards four intermediate redshift systems, viz. the lensing galaxies towards B 0218+357 ($z \sim 0.685$; Kanekar et al. 2001) and 1830-211 ($z \sim 0.886$; Chengalur et al. 1999), in addition to the two systems listed above. All four systems also give rise to well studied millimetre wavelength molecular line absorption from a host of molecules, including HCO^+. Comparing our OH data with these millimetre line transitions, we find that the linear correlation between $N_{\rm OH}$ and $N_{\rm HCO^+}$ found in molecular clouds in the Milky Way (Liszt & Lucas 1996) persists out to $z \sim 1$. It has been suggested (Liszt & Lucas 1999) that OH is a good tracer of H_2, with $N_{\rm H_2}/N_{\rm OH} \approx 10^7$ under a variety of physical conditions. We use this relationship to estimate $N_{\rm H_2}$ in these absorbers. The estimated $N_{\rm H_2}$ is $\gtrsim 10^{22}$ in all four cases and substantially different from estimates based on CO observations.

Key words. galaxies: evolution: – galaxies: formation: – galaxies: ISM – cosmology: observations – radio lines: galaxies

1. Introduction

Molecular hydrogen (H_2) is the primary constituent of the molecular component of the interstellar medium and plays a crucial role in determining the evolution of the ISM as well as the star formation rate in galaxies. For example, in the Milky Way, $M_{\rm H_2} \sim 5\times10^9 M_\odot$, comparable to the mass of the atomic component. Since it is difficult to directly detect H_2, its column density, $N_{\rm H_2}$, is usually inferred from observations of other species; these are referred to as *tracers* of H_2 (see e.g. Combes 1999 for a review). The most commonly used tracer of H_2 is CO, which is the second most abundant molecule in the ISM. Unfortunately, despite the widespread use of CO as a tracer of H_2, deducing $N_{\rm H_2}$ from CO observations remains a fairly tricky exercise (see e.g. Liszt & Lucas 1998, for a discussion).

The OH column density is known to correlate with the visual extinction A_V and, hence, with the *total* hydrogen column density, $N_{\rm H}$ (Crutcher 1979). Lucas & Liszt (1996) and Liszt & Lucas (1998, 1999) examined the variation of OH and other species (including H_2CO, HCN, HNC and C_2H) with HCO^+ and found that most molecules (except OH) showed a non-linear dependence on $N_{\rm HCO^+}$, with a rapid increase in their abundances at $N_{\rm HCO^+} \approx 10^{12}$ cm^{-2}. However, $N_{\rm OH}$ and $N_{\rm HCO^+}$ were found to have a linear relationship extending over more than two orders of magnitude in $N_{\rm HCO^+}$(Liszt & Lucas 1996), with

$$\frac{N_{\rm HCO+}}{N_{\rm OH}} \approx 0.03 \ . \qquad (1)$$

Further, the relative abundances of OH and HCO^+ to H_2 and each other were found to be constant in a variety of galactic clouds (Liszt & Lucas 1999), with $N_{\rm OH}/N_{\rm H_2} \approx 1 \times 10^{-7}$. Based on these observations, Liszt & Lucas (1999) suggested that OH and HCO^+ were good tracers of H_2.

There are presently four known molecular absorption line systems at intermediate redshifts ($z \sim 0.25-0.9$) with detected HCO^+ (Wiklind & Combes 1995, 1996a, 1996b, 1997). Until recently, OH absorption had been detected in only one of these objects, the $z \sim 0.886$ absorber towards PKS 1830-211 (Chengalur et al. 1999). We have now carried out a deep search for redshifted OH absorption in the remaining three absorbers with the GMRT, resulting in detections of absorption in all cases. In this letter, we describe our GMRT observations of two of these absorbers, viz. PKS 1413+135 ($z = 0.2467$) and B3 1504+377 ($z = 0.6734$); the OH obervations of B 0218+357 are discussed in Kanekar et al. (2001). We also compare the OH column densities obtained in the four absorbers with their HCO^+ column densities and find that the linear relationship between OH and HCO^+ found in the Milky Way persists out to moderate redshifts. Finally, we use the conversion factor suggested by Liszt & Lucas (1999) to estimate

Send offprint requests to: Nissim Kanekar
⋆ nissim@ncra.tifr.res.in
⋆⋆ chengalu@ncra.tifr.res.in

$N_{\rm H_2}$ in all these absorbers. Throughout this paper, we use $H_0 = 75$ km s^{-1} Mpc^{-1} and $q_0 = 0.5$.

2. Observations and Data analysis

The GMRT observations of PKS 1413+135 and B3 1504+377 were carried out in June and October 2001, using the standard 30-station FX correlator. This provides a fixed number of 128 spectral channels over a bandwidth which can be varied between 64 kHz and 16 MHz. We used a 4 MHz bandwidth for B3 1504+377, thus including both the 1665 and 1667 MHz OH transitions in the same band and yielding a resolution is $\sim$ 9.4 km s^{-1}. However, in the case of PKS 1413+135, the HCO$^+$ and other millimetre lines have very narrow widths. We hence used a bandwidth of 1 MHz and only observed the 1667 MHz transition (the stronger of the two lines, in thermal equilibrium), with a resolution of $\sim$ 1.75 km s^{-1}. The standard amplitude calibrators 3C48, 3C286 and 3C295 were used for both absolute flux and system bandpass calibration in both cases. No phase calibration was necessary as both PKS 1413+135 and B3 1504+377 are unresolved on even the longest baselines of the GMRT. Only thirteen and seventeen antennas were used for the final spectra of B3 1504+377 and PKS 1413+135, respectively, due to various maintenance activities and debugging; the total on-source times were 6 hours and 5.5 hours respectively.

The data were analysed in AIPS using standard procedures. Continuum emission was subtracted using the AIPS task UVLIN; spectra were then extracted in both cases by simply averaging the source visibilities together, using the AIPS task POSSM, since, as mentioned above, both sources are phase calibrators for the GMRT. Finally, the fluxes of B3 1504+377 and PKS 1413+135 were measured to be 1.2 Jy and 1.6 Jy respectively; our experience with the GMRT indicates that the flux calibration is reliable to $\sim$ 15%, in this observing mode.

The final GMRT 4 MHz spectrum towards B3 1504+377 is shown in Fig. 1[A]. No smoothing has been applied; the RMS noise is 1.3 mJy per 9.4 km s^{-1} channel. Two absorption lines can be clearly seen in the spectrum, centred at heliocentric frequencies of 995.208 MHz and 996.365 MHz. These correspond to the 1665.403 MHz and 1667.359 MHz transitions of OH, with redshifts $z_{1665} = 0.67342 \pm 0.00003$ and $z_{1667} = 0.67344 \pm 0.00003$. Note that the redshifts of the lines agree, within our error bars; we will use $z = 0.67343$, the average of the redshifts of the two lines, as the redshift of the OH absorption (but see also the discussion below). The peak line depths are 9.1 mJy and 10.0 mJy, implying peak optical depths of $\sim$ 0.76 % and 0.83 % for the 1665 and 1667 MHz transitions respectively.

The final GMRT 1 MHz spectrum towards PKS 1413+135 is shown in Fig. 1[B]. The spectrum has been Hanning smoothed and has an RMS noise of 1.3 mJy per 3.5 km s^{-1} channel. Absorption can again be clearly seen, with a peak line flux of 7.9 mJy at a heliocentric frequency of 1337.404 MHz. This can be identified with the 1667.359 MHz OH line, with a redshift $z = 0.24671 \pm 0.00001$. The peak optical depth is 0.49 %.

3. Discussion

For an optically thin cloud in thermal equilibrium, the OH column density of the absorbing gas $N_{\rm OH}$ is related to the excitation temperature T_x and the 1667 MHz optical depth τ_{1667} by the expression (e.g. Liszt & Lucas 1996)

$$N_{\rm OH} = 2.24 \times 10^{14} \left(\frac{T_x}{f}\right) \int \tau_{1667} {\rm d}V \ , \qquad (2)$$

where f is the covering factor of the absorber. In the above, $N_{\rm OH}$ is in cm^{-2}, T_x in K and dV in km s^{-1}. VLBI observations, when available, can be used to constrain the extent of the background radio continuum, and hence to estimate the covering factor f. Unfortunately, the OH excitation temperature T_x cannot be directly estimated, for cosmologically distant objects. In the Galaxy, OH emission studies have shown that this temperature may be as low as $T_x \sim T_{CMB} + 1$ K, with similar values for the HCO$^+$ line ($T_x\,(HCO^+) \sim T_{CMB}$; Lucas & Liszt 1996). However, the excitation temperatures of the redshifted HCO$^+$ lines in three of the four absorbers have been found to be *higher* than $T_{CMB}(1+z)$, the redshifted CMB temperature; it is thus quite likely that the OH excitation temperature too will be higher in these systems. Given that all four absorption systems are believed to originate either in spiral disks or in late-type galaxies (Lehár et al. 2000; Stocke et al. 1992; Stickel & Kühr 1994), we will, in the absence of additional information, assume $T_x = 10$ K, a typical temperature in dark clouds in the Milky Way.

B3 1504+377 : The OH absorption redshift, $z = 0.67343$, is in good agreement with that of the HI ($z = 0.67340$; Carilli et al. 1997); however, the molecular absorption seen in the millimetre wave bands peaks about 15 km s^{-1} away, at $z = 0.67335$ (Wiklind & Combes 1996a). Next, while the two $z = 0.67343$ OH lines are not very different in peak optical depth, the 1667 MHz line can be seen to be the wider of the two (total spread $\sim$ 103 km s^{-1} against $\sim$ 75 km s^{-1}); these widths are similar to those of the $z = 0.67335$ mm-wave lines (total spread $\sim$ 100 km s^{-1}; Wiklind & Combes 1996a). The integrated optical depths of the OH lines are $\int \tau_{1665} {\rm d}V = 0.257$ km s^{-1} and $\int \tau_{1667} {\rm d}V = 0.448$ km s^{-1}. We note that millimetre wave molecular absorption has also been detected at $z = 0.67150$ (Wiklind & Combes 1996a); the 1665 MHz OH line corresponding to this redshift arises at a heliocentric frequency of 996.352 MHz, and may thus overlap with the 1667 MHz line of the $z = 0.67343$ absorber. We will hence use the integrated optical depth in the 1665 MHz line of the $z = 0.67343$ absorber to evaluate its OH column density (assuming thermal equilibrium, i.e. $\int \tau_{1667} {\rm d}V \ / \ \int \tau_{1665} {\rm d}V = 1.8$). The integrated 1665 MHz optical depth then yields an OH column density $N_{\rm OH} = 1.04 \times (T_x/f) \times 10^{14}$ cm^{-2}. Carilli et al. (1997) estimate $f \geq 0.46$, from VLBI observations at

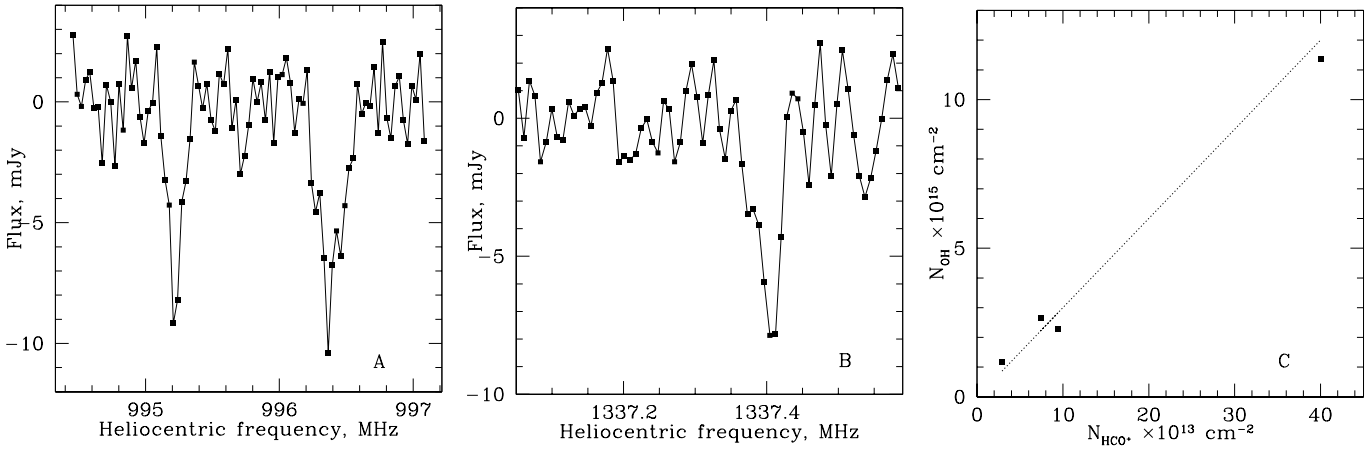


Fig. 1. [A] 9.4 km s^{-1}resolution OH spectrum towards B3 1504+377. The spectrum includes the 1665 & 1667 OH lines. [B] 3.5 km s^{-1}resolution spectrum of 1667 OH line towards PKS 1413+135. [C] $N_{\rm OH}$ versus $N_{\rm HCO^+}$ for the four absorbers of our sample. The dotted line shows the correlation found in molecular clouds in the Milky Way, and is not a fit. Note that the uncertainty in $N_{\rm OH}$ is dominated by the uncertainties in T_x and the covering factor f; the statistical errors on the optical depth are small ($< 10\%$) in all cases

Table 1. Summary of OH absorption studies

Source	z_{abs}	$N_{\rm OH}$ 10^{15} cm^{-2}	$N_{\rm HCO^+}{}^{\star}$ 10^{13} cm^{-2}	$N_{\rm HCO^+}{}^{\dagger}$ *(Obs.)* 10^{13} cm^{-2}	$N_{\rm H_2}{}^{\ddagger}$ (OH) 10^{22} cm^{-2}	$N_{\rm H_2}{}^{*}$ (CO) 10^{22} cm^{-2}	A_V
PKS 1413+135	0.24671	1.16	3.5	2.9	1.16	0.04	17.8
B3 1504+377	0.67343	2.3	6.9	9.4	2.3	0.12	27.1
B 0218+357	0.68468	2.65	7.8	7.4	2.65	40.0	28.9
PKS 1830-211	0.88582	11.38	34.2	40	11.38	4.0	123.2

* Obtained using equation 1.
† Actual measured HCO$^+$ column densities, from Wiklind & Combes 1995, 1996a, 1997, 1998 and Menten et al. 1999.
‡ Obtained using $N_{\rm H_2} = 1.0 \times 10^7 \times N_{\rm OH}$.
* Estimated from CO observations, from Wiklind & Combes 1996a, 1996b, 1997, 1999.

1.6 and 5 GHz, with the lower value obtained if only the compact core of the radio continuum (size ≈ 7.2 pc) is covered by the absorbing cloud. On the other hand, $f = 0.74$, if the radio jet of the source is also covered; this would require a cloud of size greater than ~ 54 pc. Typical sizes of Giant Molecular Clouds in the Milky Way range from 10 to 50 pc (Blitz 1990); we will hence use a covering factor $f = 0.46$ in the analysis. This yields $N_{\rm OH} = 2.3 \times 10^{15} (T_x/10)(0.46/f)$ cm^{-2}.

PKS 1413+135 : The redshift of the OH absorption towards PKS 1413+135 is in excellent agreement with that of the millimetric absorption ($z = 0.24671$; Wiklind & Combes 1997). The width of the 1667 MHz line is also quite narrow, with a total spread $\sim$ 14 km s^{-1} (slightly wider than the mm lines of Wiklind & Combes (1997), which have a total spread $\lesssim$ 10 km s^{-1}); the integrated optical depth is $\tau_{1667} = 0.023 \pm 0.001$ km s^{-1}. Equation 2 then yields an OH column density $N_{\rm OH} = 0.51 \times (T_x/f) \times 10^{14}$ cm^{-2}. VLBA maps of PKS 1413+135 at 3.6, 6, 13 and 18 cm (Perlman et al. 1996) have shown that the core (component N in their maps) is highly inverted, with a spectral index $\alpha = +1.7$. Extrapolating their flux measurements yields a core flux of ~ 70 mJy at the GMRT observing frequency, within ~ 3 mas (i.e. ~ 10 pc at $z = 0.247$). Since this is likely to be covered by the molecular cloud, we obtain a *lower* limit on the covering factor, $f \geq 0.044$. On the other hand, if components C and D (Perlman et al. 1996) are also covered, it would imply $f \sim 0.2$ (using extrapolated fluxes of components C and D). This is, however, unlikely, given that components C, D and the core are spread over ~ 20 mas (i.e. ~ 65 pc at $z = 0.247$), larger than the size of a typical molecular cloud. We will use $f = 0.044$ in the analysis (note that $f \sim 0.1$ is also possible); this yields $N_{\rm OH} = 1.16 \times 10^{15} (T_x/10)(0.044/f)$ cm^{-2}.

We also evaluate $N_{\rm OH}$ for the other two high redshift molecular absorbers in which OH absorption has been detected, towards B 0218+357 and PKS 1830-211 (Chengalur et al. 1999, Kanekar et al. 2001). In the case of PKS 1830-211, the integrated optical depth in the 1667 MHz line is $\int \tau_{1667} {\rm d}V = 1.83$ km s^{-1}; i.e. $N_{\rm OH} = 4.1 \times 10^{14} (T_x/f)$ cm^{-2}. The millimetric absorption is known to occur only towards the south-west component of the background source, which contains ~ 36 % of the radio flux (Wiklind & Combes 1998); the covering factor is thus likely to be $f \sim 0.36$. We then obtain (again using $T_x = 10$ K) $N_{\rm OH} = 11.4 \times 10^{15} (T_x/10)(0.36/f)$ cm^{-2}. Similarly, the integrated optical depth in the 1667 MHz line is $\int \tau_{1667} {\rm d}V = 0.772$ km s^{-1}, in the case of the $z = 0.6846$ absorber towards B 0218+357 (Kanekar et al. 2001); thus, $N_{\rm OH} = 1.1 \times 10^{14} \times (T_x/f)$ cm^{-2}. Carilli et al. (1993) estimate the covering factor to be $f \sim 0.4$, assuming that only component A of the background continuum source is covered by the absorbing cloud. The latter is reasonable since it is known that the millimetric absorption also only occurs against this component (Wiklind & Combes 1995). The OH column density is then $N_{\rm OH} = 2.65 \times 10^{15} (T_x/10)(0.4/f)$ cm^{-2}.

Figure 1[C] shows a plot of the OH column density versus the HCO$^+$ column density for the four absorbers of our sample. The dotted line is the relationship found in the Milky Way. All four systems lie close to this line; the linear relationship between OH and HCO$^+$ clearly appears to persist out to moderate redshifts. Table 1 summarises our results and also lists the H_2 column densities (evaluated using $N_{\rm OH}/N_{\rm H_2} = 10^{-7}$) for the four absorbers of our sample; these can be seen to be quite different from the values estimated from CO observations (penultimate column). It is interesting that our estimate of the H_2 column density in the $z = 0.6846$ absorber towards B 0218+357 is in reasonable agreement with that obtained by Gerin et al. (1997) ($N_{\rm H_2} = 2 \times 10^{22}$ cm^{-2}), using the ^{17}CO line. We also note that the good agreement between the observed HCO$^+$ column densities and those estimated using equation 1 is despite the fact that we have used the general excitation temperature, $T_x = 10$ K, for the OH line in all cases. For example, the HCO$^+$ excitation temperature is measured to be 13 K, in the case of the $z = 0.6734$ absorber towards B3 1504+377; if this value were also used for T_x, one would obtain $N_{\rm HCO^+} = 9.0 \times 10^{13}$ cm^{-2}, in even better agreement with that obtained from the HCO$^+$ absorption spectra of Wiklind & Combes (1996a).

Finally, the last column of table 1 gives the visual extinction along the four lines of sight, evaluated using the H_2 column densities of column 8, the HI column densities obtained assuming a spin temperature of 100 K (Carilli et al. 1992; Carilli et al. 1993; Carilli et al. 1997; Chengalur et al. 1999), and a Galactic extinction law ($R_V = 3.1$; Binney & Merrifield 1998). We note that a far lower extinction ($A_V \sim 28$) is obtained towards B 0218+357 than that estimated from observations of the ^{12}CO line ($A_V \gtrsim 500$; Wiklind & Combes 1999). While $A_V = 28$ is still quite large and does require the presence of fine structure in the molecular cloud (since component A is visible in the optical; Wiklind & Combes 1999), the present value requires a less dramatic change in physical conditions across the optical source than that obtained by Wiklind & Combes (1999). We also find a high extinction towards PKS 1413+135 ($A_V \sim 18$), although still somewhat smaller than that obtained from the deficit of soft X-rays ($A_V \gtrsim 30$; Stocke et al. 1992).

In summary, we find that the linear relationship between OH and HCO$^+$ column densities, seen in Galactic molecular clouds, appears to persist out to absorbers at intermediate redshift, with $N_{\rm HCO^+} \approx 0.03 \times N_{\rm OH}$. One may thus be able to use OH absorption lines to trace the H_2 content of molecular clouds at cosmological distances; all four absorbers of our sample have $N_{\rm H_2} \gtrsim 10^{22}$ cm^{-2}.

Acknowledgments The GMRT observations presented in this paper would not have been possible without the many years of dedicated effort put in by the GMRT staff to build the telescope. The GMRT is run by the National Centre for Radio Astrophysics of the Tata Institute of Fundamental Research. We thank Chris Carilli for illuminating discussions, which were useful in planning the observations.

References

Blitz L., 1990, in ASP Conf. Ser. 12, The Evolution of the Interstellar Medium, L. Blitz ed., 273
Binney J. J., Merrifield M., 1998, Galactic Astronomy, Princeton University Press, Princeton, NJ
Carilli C. L., Perlman E. S., Stocke J. T., 1992, ApJ, 400, L13
Carilli C. L., Rupen M. P., Yanny B., 1993, ApJ, 412, L59
Carilli C. L., Menten K. M., Reid M. J., Rupen M. P., 1997, ApJ, 474, L89
Chengalur J. N., de Bruyn A. G., Narasimha D., 1999, A&A, 343, L79
Combes F., 1999, in H_2 in Space, F. Combes & G. Pineau des Forts eds., Cambridge University Press, Astrophysics Series, 46
Crutcher R. M., 1979, ApJ, 239, 881
Gerin M., Phillips T. G., Benford D. J., Young K. H., Menten K. M., Frye B., 1997, ApJ, 488, L31
Kanekar N. et al., 2001, in preparation.
Lehár J. et al., 2000, ApJ, 536, 584
Liszt H., Lucas R., 1996, A&A, 314, 917
Lucas R., Liszt H., 1996, A&A, 307, 237
Liszt H., Lucas R., 1998, A&A, 339, 561
Liszt H., Lucas R., 1999, in ASP Conf. Ser. 156, Highly Redshifted Radio Lines, C. L. Carilli et al. eds., 188
Menten K. M., Carilli C. L., Reid M. J., in ASP Conf. Ser. 156, Highly Redshifted Radio Lines, C. L. Carilli et al. eds., 218
Perlman E. S., Carilli C. L., Stocke J. T., Conway J., 1996, AJ, 111, 1839
Stickel M., Kühr H., A&AS, 105, 67.
Stocke J. T., Wurtz R., Wang Q., Elston R., Jannuzi B. T., 1992, ApJ, 400, L17
Wiklind T., Combes F., 1995, A&A, 299, 382
Wiklind T., Combes F., 1996a, A&A, 315, 86
Wiklind T., Combes F., 1996b, Nature, 379, 139
Wiklind T., Combes F., 1997, A&A, 328, 48
Wiklind T., Combes F., 1998, ApJ, 500, 129

Wiklind T., Combes F., 1999, in ASP Conf. Ser. 156, Highly Redshifted Radio Lines, C. L. Carilli et al. eds., 202.